

## Biogeochemical interactions control a temporal succession in the elemental composition of marine communities

Adam C. Martiny,<sup>\*1,2</sup> Agathe Talarmin,<sup>1,4</sup> Céline Mouginot,<sup>1</sup> Jeanette A. Lee,<sup>1</sup> Jeremy S. Huang,<sup>2</sup> Alyssa G. Gellene,<sup>3</sup> David A. Caron<sup>3</sup>

<sup>1</sup>Department of Earth System Science, University of California, Irvine, California

<sup>2</sup>Department of Ecology and Evolutionary Biology, University of California, Irvine, California

<sup>3</sup>Department of Biological Sciences, University of Southern California, Los Angeles, California

<sup>4</sup>Present address: Red Sea Research Center, King Abdullah University of Science and Technology, Thuwal, Saudi Arabia

### Abstract

Recent studies have revealed clear regional differences in the particulate organic matter composition and stoichiometry of plankton communities. In contrast, less is known about potential mechanisms and patterns of temporal changes in the elemental composition of marine systems. Here, we monitored weekly changes in environmental conditions, phytoplankton abundances, and particulate organic carbon, nitrogen, and phosphorus concentrations over a 3-yr period. We found that variation in the particulate organic matter (POM) concentrations and ratios were related to seasonal oscillations of environmental conditions and phytoplankton abundances. Periods with low temperature, high nutrient concentrations and a dominance of large phytoplankton corresponded to low C : N : P and vice-versa for warmer periods during the summer and fall. In addition to seasonal changes, we observed a multiyear increase in POM C : P and N : P that might be associated with the Pacific Decadal Oscillation. Finally, there was substantial short-term variability in all factors but similar linkages between environmental variability and elemental composition as observed on seasonal and interannual time-scales. Using a feed-forward neural network, we could explain a large part of the variation in POM concentrations and ratios based on changes in environmental conditions and phytoplankton abundances. The apparent links across all time-scales between changes in physics, chemistry, phytoplankton, and POM concentrations and ratios suggest we have identified key controls of the elemental composition of marine communities in this region.

Traditionally, the elemental ratios of marine communities have been regarded as static with cellular C : N : P equal to Redfield proportions (106 : 16 : 1). However, recent studies have demonstrated extensive elemental variation depending on cellular physiological state, phylogenetic affiliation, and across major ocean regions. Cells adjust their elemental composition in response to differences in light, nutrient availability, and other environmental factors (Rhee 1978; Goldman et al. 1979; Goldman and Dennett 2000; Leonardos and Geider 2004; Mouginot et al. 2015). This includes elevated C : P and N : P under P limited growth and lower ratios under N limitation or nutrient replete conditions. Plankton lineages can also have unique elemental composition (Quigg et al. 2003; Zimmerman et al. 2014a). For example, small marine Cyanobacteria have elevated C : P and N : P in comparison to larger eukaryotes like diatoms (Arrigo et al. 2002; Martiny et al. 2013a). Finally, there are clear

regional differences in the elemental composition of marine communities, whereby the warm, nutrient depleted oligotrophic gyres have elevated carbon-to-nutrient ratios, lower ratios in nutrient replete upper latitude waters, and near Redfield proportions in upwelling regions (Martiny et al. 2013a,b; Teng et al. 2014). This regional variability appears to be driven by a combination of changes in environmental conditions, cellular physiologies, and community structure (Weber and Deutsch 2010; Martiny et al. 2013a; Zimmerman et al. 2014b). In contrast, we know little about potential mechanisms and patterns of *temporal* changes in the elemental composition and stoichiometry in marine systems.

Many ocean regions display strong temporal changes in physical, chemical, and biological factors (Church et al. 2013). One example is the eastern boundary California Current system, where many oceanographic factors vary seasonally (Legaard and Thomas 2006; Venrick 2012). Temperature is commonly lower during the winter and spring and elevated during the summer and fall. Related, nutrient

\*Correspondence: amartiny@uci.edu

availability is higher during the winter and spring due to a combination of low overall utilization, mixing, and upwelling followed by limited nutrient availability during the summer and fall months. In addition to these seasonal changes, the system is broadly characterized by intermediate temperatures, high nutrient supply rate but low nitrate:phosphate (Schnetzer et al. 2013), and high nitrate: iron supply ratios (King and Barbeau 2011)—in part due to upwelling. These chemical and physical changes can also influence the abundances of different phytoplankton groups.

Superimposed on such seasonal changes, coastal environments experience short-term episodic (e.g., tidal changes) as well as stochastic event (e.g., rain, river runoffs, and eddies). There may also be variability in the length of alternate phases of upwelling winds and relaxation contributing to the initiation and intensity of phytoplankton blooms in the region (Kudela et al. 2006). The California Current also experiences interannual environmental changes including ENSO and Pacific Decadal Oscillation (PDO) (Rykaczewski and Checkley 2008). Such short and long-term environmental drivers can have strong impacts on the ocean chemistry, plankton populations, and activity (Rebstock 2003; Allison et al. 2012; Hatosy et al. 2013; Martz et al. 2014) and perhaps the elemental composition and ratios of marine communities.

Here, we quantify physical and chemical oceanographic factors, phytoplankton abundances across a range of taxa, and the elemental composition and ratios of particles at the coastal “Microbes in the Coastal Region of Orange County” (MICRO) site in the southern section of the California Current ecosystem (Allison et al. 2012). We hypothesize that changes in environmental conditions and associated phytoplankton abundances lead to predictable elemental composition and ratios of marine communities. Linkages between environmental, biological, and particulate matter factors are hypothesized to manifest themselves across interannual, seasonal, and short time-scales. This leads to a series of predictions for this site: First, we predict elevated temperatures and low nutrient concentrations during the summer and fall and vice-versa during winter and spring. Second, these environmental changes lead to higher abundances of the larger-sized diatoms during the winter and spring. This will be followed by increased concentrations of dinoflagellates, small eukaryotic phytoplankton during the late spring and summer, whereas *Synechococcus* and *Prochlorococcus* will have peak abundances in the summer and fall. Third, a seasonal succession of environmental conditions and phytoplankton abundances will influence POM concentrations, which we predict to be highest during bloom conditions in the spring. Fourth, changes in physical, chemical and biological factors lead to systematic variation in the particulate C : P and N : P with elevated ratios during the summer and fall—analogueous to what has been observed spatially (Martiny et al. 2013a). In

addition to seasonal changes, we predict a multiyear mean elemental stoichiometry near Redfield proportions as has been observed in other upwelling regions (Martiny et al. 2013a). Finally, we expect extensive interannual and short-term variability in the elemental composition ratios—tied to similar environmental and biological factors as on other time scales.

## Materials and methods

### Location and sampling

Surface water from the “Microbes in the Coastal Region of Orange County” (MICRO) time series station at Newport Pier (33°36.37'N, 117°55.87'W) was collected weekly, in the morning, from 11 January 2012 to 7 January 2015. One liter polycarbonate bottles rinsed three times prior to sampling were filled for quantification of POM and nutrient concentrations (three samples each from two bottles for a total of six replicates). A 15 mL rinsed Falcon tube was filled for flow cytometry analyses. All samples were further processed in the laboratory within 2 h of collection. Temperature and salinity were continuously monitored using an automated shore station mounted next to the sampling site ([www.sccoos.org](http://www.sccoos.org)).

### Nutrient measurements

Nitrate and phosphate samples were collected in pre-washed 50 mL Falcon tubes by filtration through a 0.2  $\mu\text{m}$  syringe filter and stored at  $-20^{\circ}\text{C}$  until further analysis. Soluble reactive phosphorus (SRP) concentrations were determined using the magnesium induced coprecipitation (MAGIC) protocol and calculated against a potassium monobasic phosphate standard (Lomas et al. 2010). Nitrate samples were treated with a solution of ethylenediaminetetraacetate and passed through a column of copperized cadmium fillings (<http://bats.bios.edu/methods/chapter9.pdf>). We also collected weekly ammonia samples by adding 0.2  $\mu\text{m}$ -filtered seawater to 20 mL plastic scintillation vials that were prewashed with 5% HCl and rinsed three times with the 0.2  $\mu\text{m}$ -filtered seawater samples. Ammonia samples were frozen at  $-20^{\circ}\text{C}$  at the laboratory, until processing at the Marine Sciences Institute Analytical Lab at UCSB using flow injection analysis. Detection limits of ammonia, nitrate, and phosphate measurements were 100  $\text{nmol L}^{-1}$ , 80  $\text{nmol L}^{-1}$ , and 40  $\text{nmol L}^{-1}$ , respectively.

### Particulate organic matter

Twelve replicate 300 mL seawater samples were filtered onto precombusted ( $500^{\circ}\text{C}$ , 5 h) GF/F filters (Whatman, Florham Park, New Jersey) for particulate organic carbon (POC) and nitrogen (PON) or phosphorus (POP) concentrations. After filtration, six filters for POP were dried at  $65^{\circ}\text{C}$  for 1 d and stored at  $-20^{\circ}\text{C}$  until further analysis, while six filters for POC + PON were directly frozen. Then, POP filters were thawed and processed using a modified ash-hydrolysis method (Lomas et al. 2010). After thawing, POC/PON filters

were allowed to dry overnight at 65°C before being packed into a 30 mm tin capsule (CE Elantech, Lakewood, New Jersey). Samples were then analyzed for C and N content on a FlashEA 1112 nitrogen and carbon analyzer (Thermo Scientific, Waltham, Massachusetts), following the protocol of Sharp (1974). POC and PON concentrations were calibrated using known quantities of atropine.

### Phytoplankton cell counts

Samples for flow cytometry analyses were fixed with pre-filtered paraformaldehyde (0.5% final concentration) and subsequently incubated at 4°C for 30 min, flash frozen in liquid nitrogen, and stored at -80°C until further processing. On thawing, samples were prescreened through custom 20  $\mu\text{m}$  nylon mesh equipped caps fitting the 5 mL polypropylene FACS tubes to remove large particles and increase the signal to noise ratio. Samples were analyzed on an Influx V7 FACS machine (Becton Dickinson, San Jose, California) (Lomas et al. 2010). Briefly, we quantified *Prochlorococcus*, *Synechococcus*, and pico/nano-eukaryotic phytoplankton (PNE) based on the forward and side scatter, red fluorescence for chlorophyll *a* ( $692 \pm 45$  nm), orange fluorescence for phycoerythrin ( $580 \pm 30$  nm) after excitation with a Coherent Sapphire solid-state 488 nm laser (200 mW). Yellow-green beads (1  $\mu\text{m}$ , Spherotech, Lake Forest, Illinois) were systematically added to the samples and acquisitions lasted 4 min. The flow rate ( $\sim 23 \mu\text{L min}^{-1}$ ) was estimated by weighing each tube before and after acquisition. Data were further analyzed using FCS Express version 4 Research RUO (Denovo Softwares, Los Angeles, California).

Samples for characterizing the microphytoplankton community composition were preserved using 10% formalin (final conc. 1%) and examined by inverted light microscopy (400X), after settling 25 mL in Utermöhl chambers for 24 h. Forty fields of view were counted, giving a limit of detection of 3000 cells  $\text{L}^{-1}$ . Lineages including *Akashiwo sanguinea*, *Alexandrium* spp., *Dinophysis* spp., *Lingulodinium polyedrum*, *Prorocentrum* spp., *Pseudo-nitzschia* spp. and broadly diatoms and other dinoflagellates were enumerated (Seubert et al. 2013). These were subsequently combined into total dinoflagellates and diatoms.

### Biomass estimation

For *Synechococcus* and PNE cells, we estimated the carbon cell quota directly using flow cytometry-based cell sorting followed by carbon elemental analysis. Seawater samples were prescreened on a 20  $\mu\text{m}$  nylon mesh and gently pre-concentrated on a polycarbonate 0.22- $\mu\text{m}$  membrane while avoiding exposing the filter to the air. Filtration was stopped and cells were gently resuspended in the remaining 5 mL and screened again on a 20  $\mu\text{m}$  nylon mesh before processing. Samples were then sorted using a BD Influx cell sorter at a pressure less than 0.07 bar higher than the sheath fluid (1.86 bar) through a 70  $\mu\text{m}$  ceramic nozzle tip. Sorting at a rate of 2000–10,000 events  $\text{s}^{-1}$  resulted in purity > 97% (proportion of targeted events in sorted cells as estimated by

microscopy). A minimum of  $3 \times 10^5$  PNE ( $n = 9$ ) and  $5 \times 10^6$  *Synechococcus* ( $n = 7$ ) cells were sorted before carbon content estimation. Sorted cells were collected and stored at 4°C until filtration (within 5 h) onto 13 mm precombusted (450°C, 4 h) 0.3  $\mu\text{m}$  (GF/75) and 0.7  $\mu\text{m}$  (GF/F) glass fiber filters for *Synechococcus* and PNE, respectively. Each fraction was rinsed three times with 0.22  $\mu\text{m}$  filtered sheath fluid, which was also used to obtain blanks. Filters were dried overnight at 60°C and stored at -20°C, until further analysis. The carbon content was quantified on a COSTECH Analytical Technologies, EAS4010 unit with detection limits of  $\sim 0.3$  ug/sample for C and  $\sim 0.2$  ug/sample for N (Casey et al. 2013).

We estimated a constant C biomass for *Prochlorococcus*, dinoflagellates and diatoms to 78 fg, 3 ng, and 0.5 ng, respectively, from past studies (Brzezinski 1985; Menden-Deur and Lessard 2000; Casey et al. 2013).

### Data analysis

All data analyses were done in MATLAB unless otherwise noted. We applied the Lomb-Scargle algorithm to determine the spectral periodogram of each factor using uninterpolated data and subsequently localized maxima between 0.8  $\text{yr}^{-1}$  and 1.2  $\text{yr}^{-1}$  cycles (Scargle 1982). Temporal decomposition of the data was done by (1) estimating the linear interannual trend, (2) quantifying the monthly mean after removal of any interannual trend, and (3) applying a single time-step differencing to interannually and seasonally detrended data, followed by spearman correlation (Chatfield 2013).

We used a multivariate time-delay neural network analysis with three nodes and up to two time lag steps to quantify the partial contribution of environmental and biological factors to the variability of concentrations and ratios of POM. As multiple parameters were strongly covarying, we evaluated the partial contribution of temperature, nitrate, ammonia, *Prochlorococcus*, PNE, and diatoms. First, we used 70%, 15%, and 15% of the observations as training, validation, and targets, respectively. Optimization of the network was evaluated using bayesian regularization (Hagan et al. 1996). The mean neural network model Pearson correlation coefficients across 10 ensemble were:  $R_{\text{POP}} = 0.51$ ,  $R_{\text{PON}} = 0.39$ ,  $R_{\text{POC}} = 0.40$ ,  $R_{\text{C} : \text{N}} = 0.47$ ,  $R_{\text{C} : \text{P}} = 0.51$ ,  $R_{\text{N} : \text{P}} = 0.54$ . Second, we converted the neural network into a closed loop and sequentially varied each factor between the minimum and maximum observed values (50 steps), while keeping all other factors at mean observed value to isolate the partial effect. This procedure was repeated across 10 ensembles and the mean and standard deviation for the output value (POM concentrations or ratios) were reported.

### Results

We wanted to evaluate our hypothesis that this region of the California Current ecosystem experienced systematic

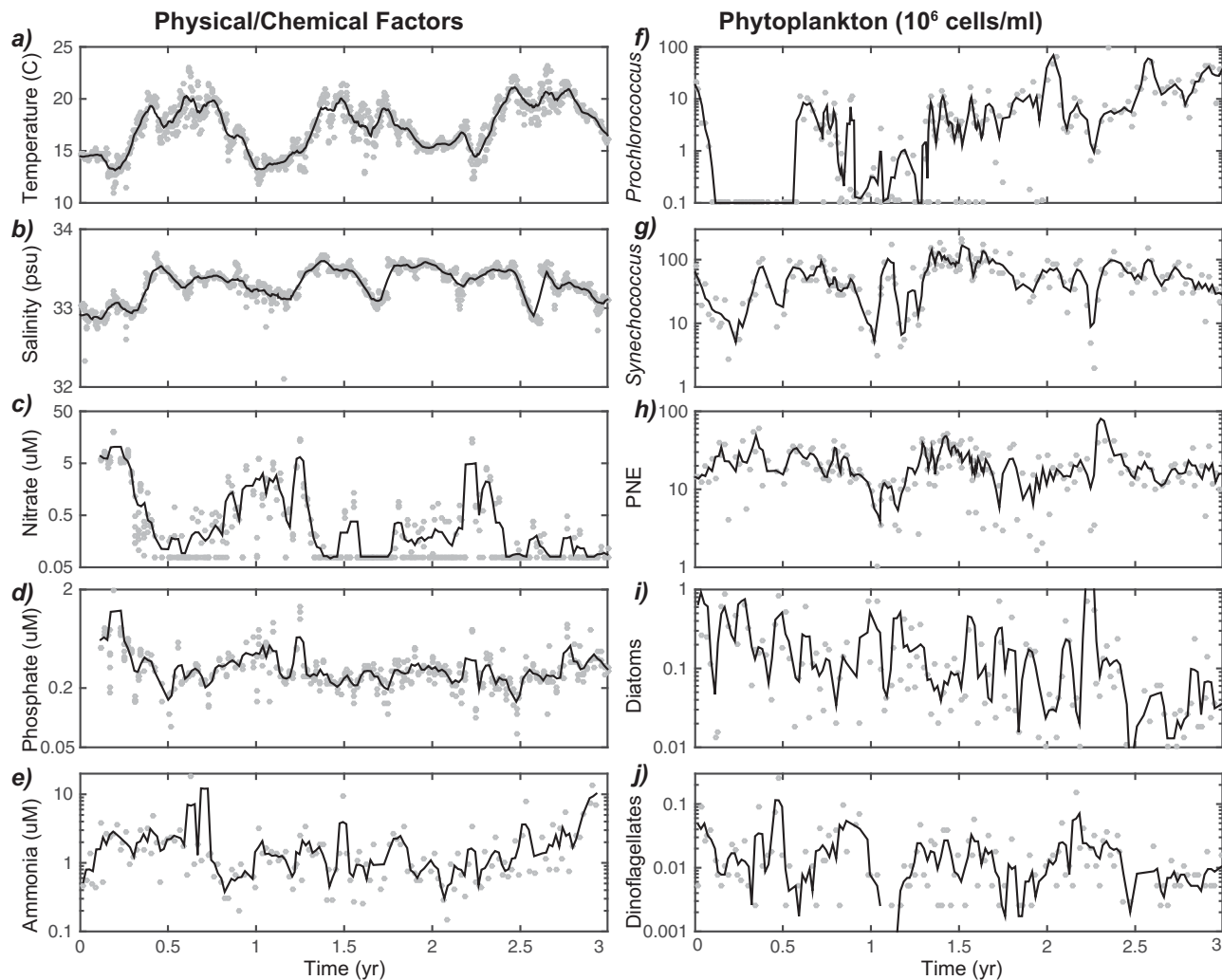


**Fig. 1.** Temporal variability in physical, chemical, and biological factors at the MICRO site including (a) temperature (daily values), (b) salinity (daily values), (c) nitrate, (d) phosphate, (e) ammonia, (f) *Prochlorococcus*, (g) *Synechococcus*, (h) pico/nano-eukaryotic phytoplankton (PNE), (i) dinoflagellates, and (j) diatoms. Lines represent 28 d moving averages.

changes in environmental conditions and associated phytoplankton abundances that subsequently lead to consistent variation in the elemental composition and ratios of marine communities across time-scales. To test this hypothesis, we measured physical (temperature and salinity), chemical (phosphate, nitrate, and ammonia), and biological (abundances of *Prochlorococcus*, *Synechococcus*, pico/nano-eukaryotic phytoplankton (PNE), diatom and dinoflagellate lineages) parameters (Fig. 1), as well as the particulate organic phosphorus (POP), nitrogen (PON), and carbon (POC) concentrations and ratios (referred to as C : N, and C : P, N : P hereafter) over a 3-yr period (Fig. 2). Most ocean factors will likely display some annual oscillation and thus be auto-correlated. To overcome this, we linearly decomposed each factor into possible seasonal, interannual, and short-term components and examined the resulting trends and correlations (Table 1).

### Seasonal cycling

We observed strong seasonal cycling in environmental conditions, whereby multiple factors displayed significant annual oscillations (Figs. 1, 3). Temperature was 2°C above average from June to October and vice-versa from January through April (Figs. 1a, 3a, 4a). An opposite phased annual oscillation was observed for macronutrients (i.e., nitrate and phosphate), where the concentrations reached maxima in April and minima during the summer and fall (Figs. 1c,d, 3b,c, 4a). In contrast, neither salinity nor ammonia displayed significant seasonal cycles (Figs. 1b,e, 3d).

The abundances of phytoplankton lineages also displayed significant seasonal successions (Figs. 1f–j, 3e–i). In accordance with our prediction, diatoms reached peak abundance in April (Figs. 1i, 4b). Similarly, dinoflagellates and PNE were also more frequent earlier in the year and had maximum abundances between March and June (Figs. 1h,j, 4b). The

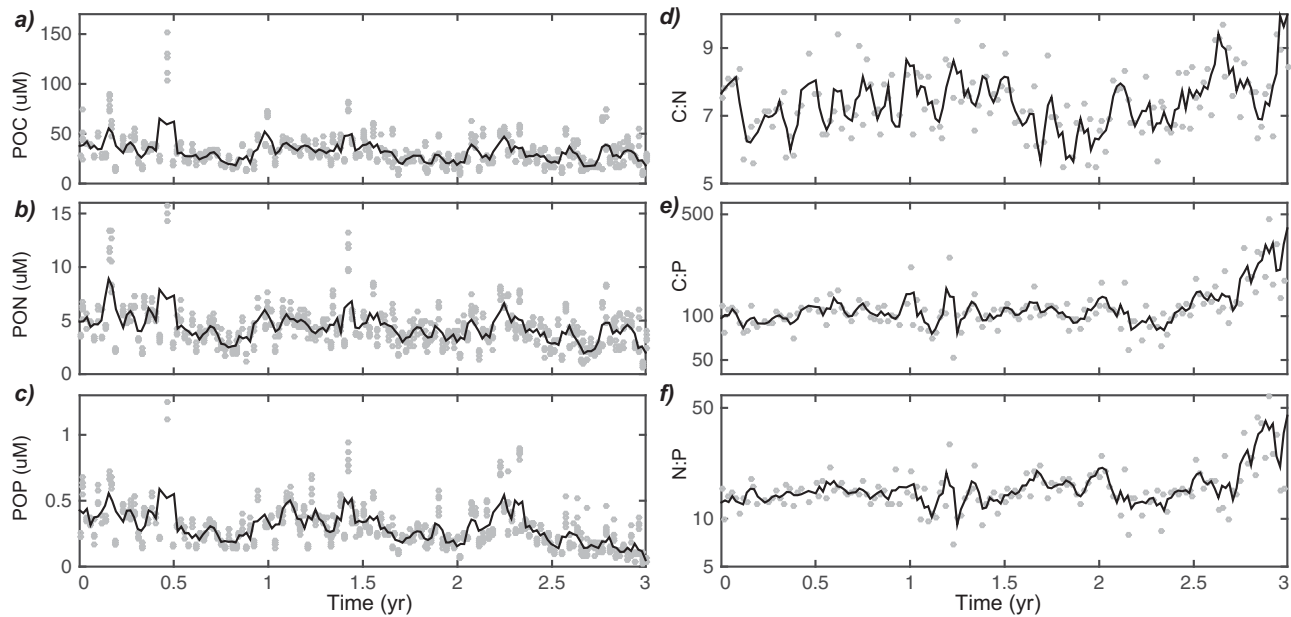


**Fig. 2.** Temporal variability in particulate organic matter and their molar ratios including (a) particulate organic phosphorus (POP), (b) particulate organic nitrogen (PON), (c) particulate organic carbon (POC), (d) C : N, (e) C : P, and (f) N : P. All ratios are molar and represent the ratio of the mean POM values for each time point. Lines represent 28 d moving averages.

**Table 1.** Overview linear model\* parameter and contribution to variance

Factors	Linear model (interannual)				ANOVA				
	Slope	Std. error	t-value	p	Interannual SQ	p	Month SQ	p	Residual SQ
Temperature	0.0020	0.0004	5.5	$1 \times 10^{-7}$	128	$2 \times 10^{-14}$	596	$3 \times 10^{-32}$	255
Salinity	0.0001	0.0001	2.2	0.03	0.3	$3 \times 10^{-3}$	1.5	$7 \times 10^{-5}$	5.1
Phosphate	-0.0002	0.0001	-3.2	$2 \times 10^{-3}$	0.7	$2 \times 10^{-4}$	1.7	$1.3 \times 10^{-3}$	7.3
Nitrate	-0.0028	0.0006	-4.4	$2 \times 10^{-5}$	197	$2 \times 10^{-8}$	342	$2 \times 10^{-7}$	809
Ammonia	0.0005	0.0008	0.7	0.50	25	0.1	155	0.12	$1.3 \times 10^3$
PNE	-1.5	4.1	-0.4	0.71	$1 \times 10^8$	0.4	$6 \times 10^9$	$9 \times 10^{-3}$	$3 \times 10^{10}$
Prochloro.	21.7	3.3	6.5	$1 \times 10^{-9}$	$8 \times 10^9$	$1 \times 10^{-10}$	$6 \times 10^9$	$3 \times 10^{-4}$	$2 \times 10^{10}$
Synecho.	26.7	8.8	3.0	$3 \times 10^{-3}$	$1 \times 10^{10}$	$4 \times 10^{-3}$	$7 \times 10^{10}$	$2 \times 10^{-7}$	$1 \times 10^{11}$
Dino.	-15.9	6.1	-2.6	0.01	$4 \times 10^9$	$8 \times 10^{-3}$	$3 \times 10^9$	0.9	$8 \times 10^{10}$
Diatom	-197.9	86	-2.3	0.02	$1 \times 10^{12}$	$2 \times 10^{-3}$	$4 \times 10^{12}$	$5 \times 10^{-4}$	$2 \times 10^{13}$
POP	-0.0001	0.0000	-3.7	$3 \times 10^{-4}$	0.6	$6 \times 10^{-7}$	0.8	$1 \times 10^{-4}$	2.9
PON	-0.0014	0.0005	-2.9	$5 \times 10^{-3}$	47	$2 \times 10^{-4}$	71	0.03	467
POC	-0.0090	0.0038	-2.3	0.02	$2 \times 10^3$	$1.5 \times 10^{-3}$	$4.7 \times 10^3$	0.03	$3 \times 10^4$
C : N	0.0005	0.0003	1.8	0.08	3.4	0.1	11	0.6	166
C : P	0.0687	0.016	4.4	$2 \times 10^{-5}$	$9 \times 10^4$	$8 \times 10^{-7}$	$5 \times 10^4$	0.2	$5 \times 10^5$
N : P	0.0078	0.0019	4.1	$6 \times 10^{-5}$	$1 \times 10^3$	$1 \times 10^{-6}$	877	0.10	$7 \times 10^3$

\*The linear model including both an interannual and monthly contribution. The coefficients for the monthly contributions (12 factors) are visualized in Fig. 4 and not shown here. The unit for the slope is var unit  $\times$  d<sup>-1</sup>.

smaller *Synechococcus* sustained elevated concentrations from the early summer into fall but was observed at lower concentration in the late winter (Figs. 1g, 4b). *Prochlorococcus*—the smallest phytoplankton lineage—reached elevated concentrations during short periods in the late summer and into

the fall (Figs. 1f, 4b). Thus, the phytoplankton community composition followed a successional pattern starting with early blooms of diatoms, followed by dinoflagellates and then PNE, whereas later in the season *Synechococcus* and then *Prochlorococcus* were more frequent (Fig. 4b).

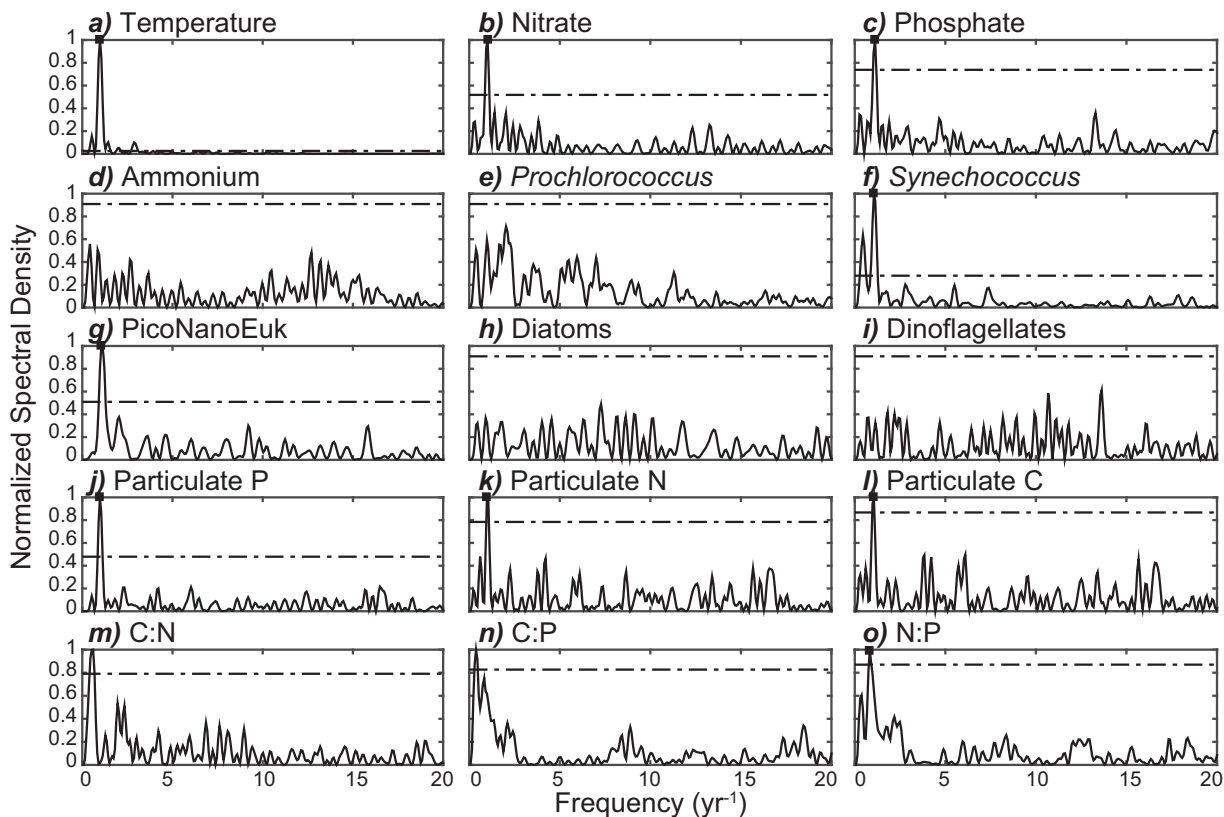


**Fig. 3.** Periodogram of all factors. The frequency distribution was estimated using the Lomb-Scargle algorithm (Scargle 1982) and the dashed line represents the 90% power-level threshold. Peaks above this threshold and a frequency within  $0.8\text{--}1.2\text{ yr}^{-1}$  are marked.

POM concentrations showed significant and synchronous seasonal cycling, too (Figs. 2a–c, 3j–l). As predicted, POM concentrations were high from March into July and reached a minimum in the late fall (Fig. 4c). The median particulate C : N : P were  $107 : 14.7 : 1$  and thus close to Redfield proportions. In addition, C : P and N : P ratios showed seasonal changes (Figs. 2e,f, 3n,o) and were lower during the spring and peaked by the end of fall (Fig. 4d). C : N had less seasonal variability (Figs. 2d, 3m, 4d).

### Interannual trends

We observed significant interannual trends across environmental conditions, phytoplankton abundances, and the elemental composition and ratios of marine communities (Table 1; Fig. 4e–h). Over the 3-yr sampling period, the annual mean temperature rose by  $\sim 2^\circ\text{C}$  (Table 1; Fig. 4e). Nitrate and phosphate concentrations showed orthogonal changes and the mean concentrations dropped by  $3\ \mu\text{M}$  and  $0.22\ \mu\text{M}$ , respectively (Table 1). In contrast, we saw a slight increase in ammonia concentrations (Fig. 4e). Phytoplankton populations also displayed long-term trends, whereby eukaryotic lineages declined and Cyanobacteria increased in abundances (Fig. 4f). The concentrations of POC, PON, and POP decreased during this period with the strongest decline

in POP (Fig. 4g). This led to a multiyear increase in C : P and N : P but not C : N (Fig. 4h).

### Short-term changes

In addition to the described seasonal and interannual trends, we also detected extensive short-term variability across all factors (Figs. 1, 2). Most factors displayed significant autocorrelation at the weekly time-scale. Thus, we removed the interannual and seasonal variability and then applied a single time-step differencing. This allowed us to examine linkages between short-term changes (and not absolute values) between factors (Fig. 5). We observed many similar trends as for other time-scales. This included significant negative correlations between temperature and concentrations of nitrate and phosphate. Temperature further had a direct effect on several phytoplankton lineages (positive for *Synechococcus* and negative for dinoflagellates). Dinoflagellates also appeared negatively affected by salinity, whereas nutrients had little effect. The distribution of several lineages was also related as Cyanobacteria and PNE showed positive correlations.

Several factors also influenced short-term changes in POM concentrations and ratios (Fig. 5). Temperature had a negative effect on POP and PON, whereas nutrients had the opposite effects. This led to a direct positive

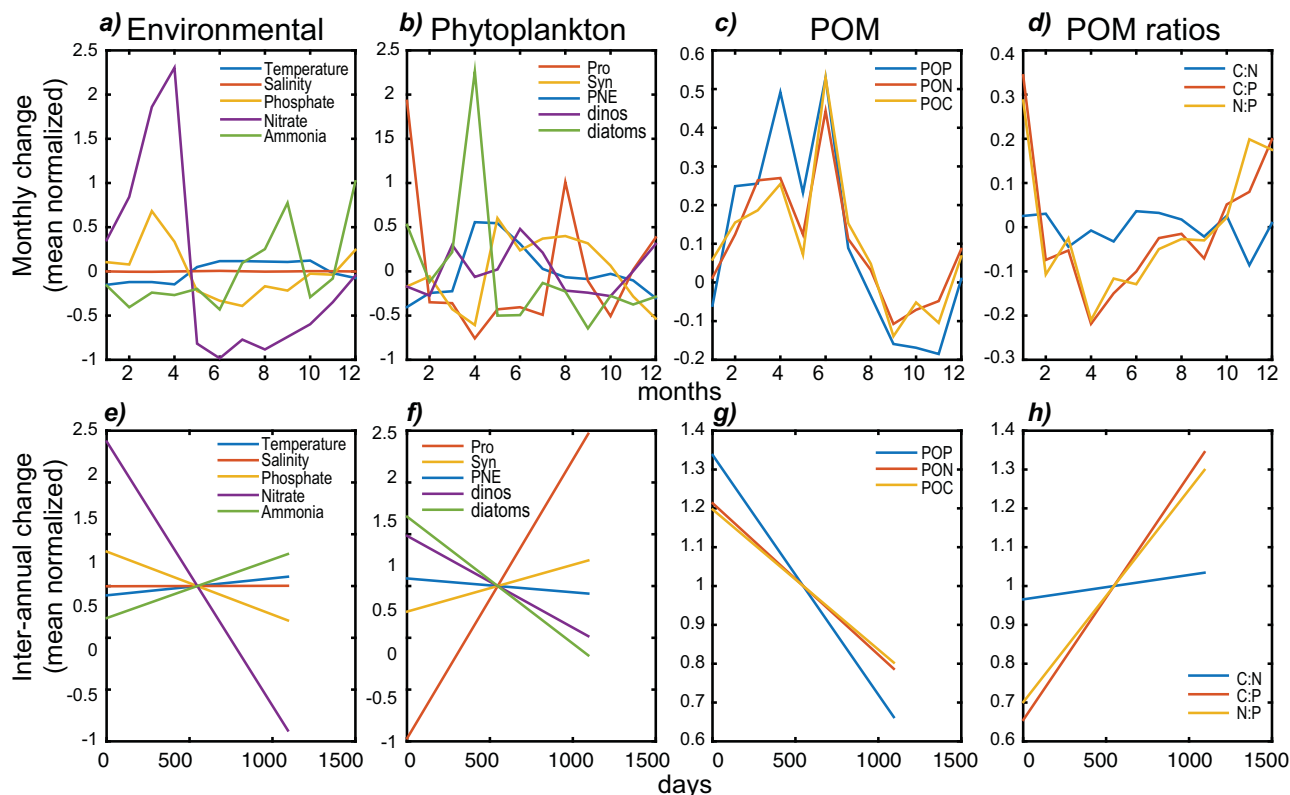


**Fig. 4.** Seasonal (a–d) and interannual (e–h) contributions to the variability across environmental (a and e), biological (b and f), particulate organic matter (POM) (c and g), and POM molar ratios (d and h). The interannual graphs represent linear trend lines through the full dataset, whereas the seasonal contributions are estimated as the mean of the corresponding month of the full dataset minus the interannual trend. Each factor was normalized to the mean value and unitless.

temperature (and negative for nitrate) effect on C : P. Whereas salinity did not seem to display strong seasonal oscillation (Fig. 3) or interannual variability, we did see a direct short-term negative salinity effect across POM concentrations but not ratios. Eukaryotic phytoplankton populations (PNE and diatoms) also had positive correlations with POM concentrations. POC, PON, and POP showed very high intercorrelations at short time-scales. As we used different analytical techniques to measure POP vs. POC + PON, these correlations suggest that external factors and not measurement errors led to short-term changes in POM concentrations. POP displayed stronger seasonal and long-term trends compared with POC or PON. Further, we observed that both the C : P and N : P were correlated to POP concentrations at short time-scale. Thus, it appeared variability in POP was the key driver for these two ratios. Similarly, we observed that POC but not PON was significantly correlated to C : N and thus suggested that C : N levels were primarily driven by changes in POC concentrations.

#### Predicting POM concentrations and ratios

Our analyses identified multiple factors putatively influencing the temporal evolution of the elemental composition

of marine communities. We next used multivariate time-delay neural network analyses to predict the POM concentrations and ratios. We found that optimal combinations of environmental and biological factors could predict the elemental composition across the 3-yr period with  $R_{\text{Pearson}}$  ranging from 0.39 to 0.56. We also identified the partial effect of each environmental and biological factor and thus quantifying the direct influence on the POM concentrations and C : N : P (Fig. 6). The contributions supported the observations in the time-series decomposition analysis, whereby increases in temperature and prokaryotic phytoplankton led to lower POM concentrations and elevated ratios and vice-versa for ammonia, nitrate, and large phytoplankton types. We also identified how increases in diatom abundances resulted in higher C : N.

#### Biomass contribution

Lastly, we estimated the biomass contribution from each measured phytoplankton group over the 3-yr period (Fig. 7). We directly measured the biomass of *Synechococcus* and PNE using a combination of cell sorting and elemental analysis. The measured phytoplankton groups contributed an average of 59% to total POC (Fig. 7A). PNE and diatoms contributed the most, followed by dinoflagellates, *Synechococcus*, and a

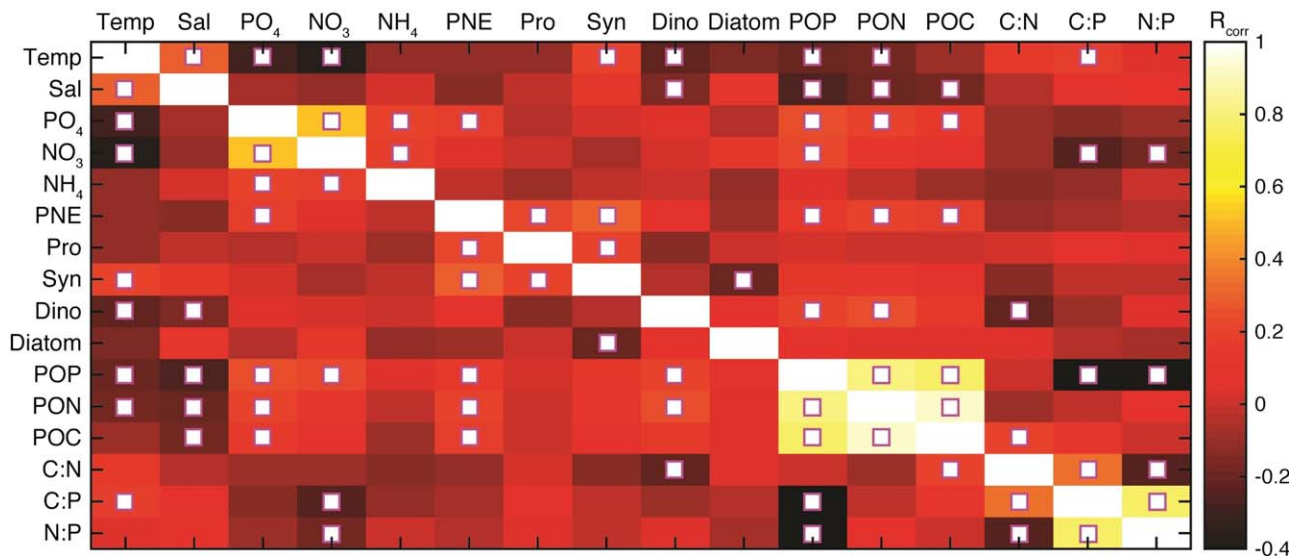


**Fig. 5.** Correspondence of short-term temporal changes between factors using Spearman correlation. White squares represent correlations at  $p < 0.05$ .

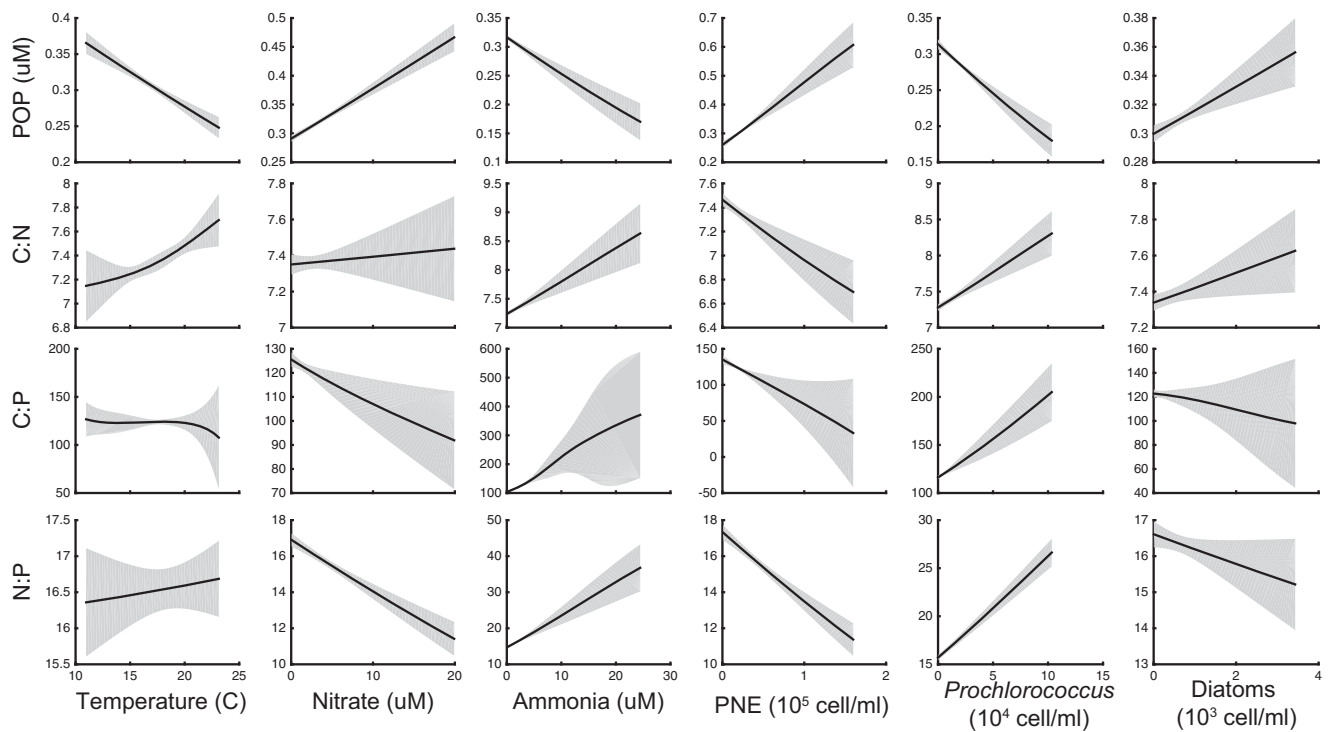


**Fig. 6.** Contribution of six environmental factors to variation in particulate organic matter and molar ratios. The nonlinear partial contribution is estimated using a time-delay neural network by varying the input factor while keeping all other factors at their observed level. The shaded areas represent the standard deviation across 10 ensemble runs.

minuscule contribution by *Prochlorococcus*. However, we also saw considerable temporal variability and at some time points, up to 90% of POC could be associated with unknown fractions (Fig. 7B).

**Discussion**

Overall, we find strong support for our hypotheses and associated predictions and see clear temporal changes in POM concentrations and ratios and thus not static. In line



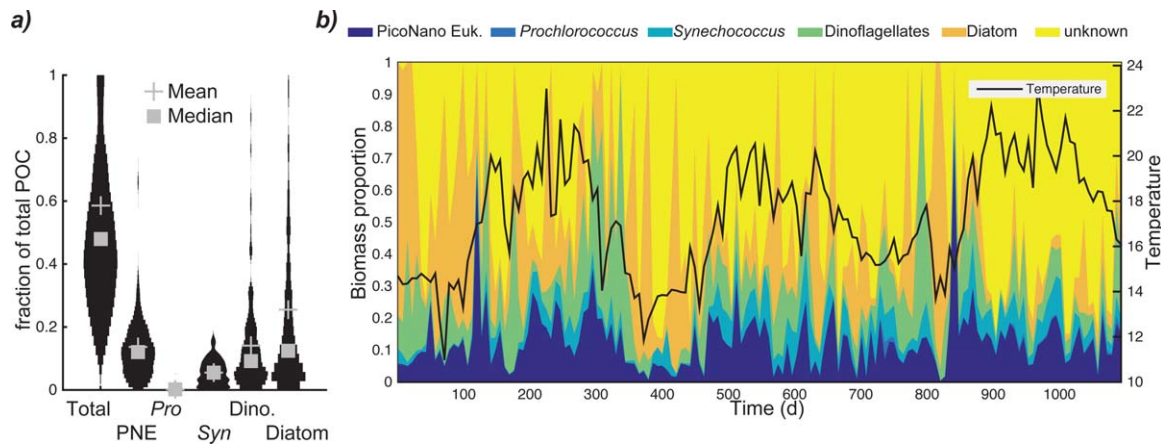


**Fig. 7.** Biomass contribution of all as well as individual phytoplankton groups to total particulate organic carbon (POC). **(a)** Violin plot of fraction of total POC and **(b)** temporal variation in contribution to total POC. Carbon cell quota of *Prochlorococcus*, *Synechococcus*, pico/nano-eukaryotic phytoplankton (PNE), dinoflagellates, and diatoms were 78 fg, 120 fg, 1974 fg, 3 ng, and 0.5 ng, respectively.

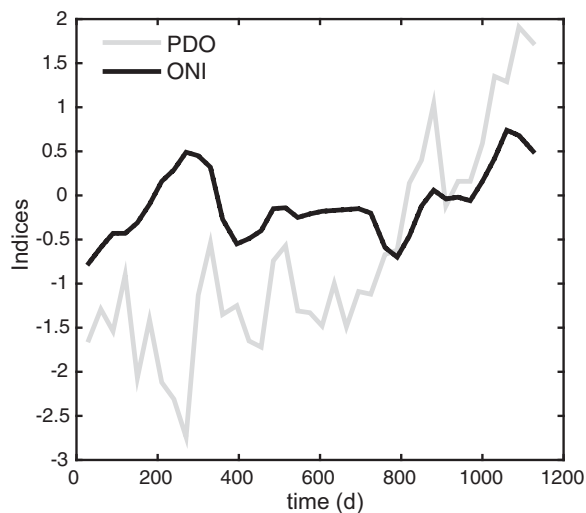


**Fig. 8.** PDO and ONI index values retrieved from NOAA's National Climatic Data Center.

with previous studies (e.g., Hulburt et al. 1960; Menzel and Ryther 1960), cycles in the environmental conditions are likely causing a seasonal succession in the phytoplankton community structure. Changes in the physics, chemistry, and biology correspond to seasonal oscillations in the particulate organic matter, whereby the concentrations are elevated following periods with higher nutrients and dominance by eukaryotic phytoplankton. As POP oscillates more strongly, we also observe seasonally changing elemental ratios. Elevated C : P and N : P are in the fall are associated with high temperature, low nutrients, and a dominance of small phytoplankton and vice-versa during the late winter and spring. Apparent linkages at both interannual and short-term time-scales corroborate the seasonal pattern, whereby parallel changes in temperature, nutrients, and phytoplank-

ton community structure lead to changes in POM concentrations and ratios. As many environmental factors show extensive interannual and weekly changes, this in turn causes at least part of the observed variability in the elemental composition of the overall community. These linkages are confirmed using a time-delay neural network demonstrating we can broadly predict changes in C : N : P in this area.

Even though these are only correlation patterns, the apparent link between changes in physics, chemistry, and biology with POM concentrations and ratios are consistent with previously observed spatial patterns (Martiny et al. 2013a). From spatial patterns, we should expect a multiyear average C : N : P close to 106 : 16 : 1 in lower latitude upwelling regions, which is close to the observed 107 : 15 : 1. However, the elemental ratios are not static in time as periods of increased temperature, low macronutrient availability, and a dominance of smaller phytoplankton lineages are connected to elevated ratios. This matches regional observations of elevated ratios in the gyres and suggests we have identified key controls of the elemental composition of marine communities in this region.

During the 3-yr period, we detect a strong upward trend in temperature. This temperature increase may be associated with broader shifts in the Pacific Ocean. The underlying climatic cause is currently unknown but the temperature change coincides with a shift in the Pacific Decadal Oscillation (PDO), which has gone from a negative to positive mode between 2012 and 2015 (Fig. 8). During the positive mode, California Current waters display a positive temperature anomaly (Biondi et al. 2001; Mantua and Hare 2002) and changes in the PDO can have substantial impact on the marine trophic structure. The temperature shift could also be related to ENSO or other basin-wide ocean phenomena but such alternative links appear weak and PDO shows the

highest correlation to our data (Fig. 8). Likely connected to the upward shift in temperature, we saw a big decline in nutrient inventories and major shifts in the phytoplankton community structure (Fig. 4e–h). These shifts in turn lead to a ~30% increase in C : P and N : P in this system. Regardless of the climatic cause, our data suggests that long-term upward shifts in temperature and associated changes in nutrients and phytoplankton can have profound impacts on elemental ratios in this marine ecosystem.

In support of past studies conducted in this area (Legaard and Thomas 2007; Allison et al. 2012; Hatosy et al. 2013), we also detect extensive short-term variability across physical, chemical, and biological factors. This weekly variability in conditions influences the elemental composition and ratios and can be locally driven by shifting water masses, fast community turnover, or cellular elemental plasticity (Allison et al. 2012; Mouginot et al. 2015). As an example, we observed a 4-week bloom of *Prochlorococcus* reaching  $1 \times 10^5$  cells mL<sup>-1</sup> during January 2014. This was unexpected due to the low temperature (~15°C) but corresponded to elevated C : P (~170) and N : P (~24) ratios during this period and may be connected to advection of water masses from lower latitude regions.

Based on a combination of direct and literature estimates of cellular biomass, the measured phytoplankton groups constitute ~59% of the particulate organic material. Combined with various heterotrophic groups, these observations suggest that detritus and terrestrially derived particles constitute a minority of POC in this area. But our data also revealed periods, where most of the POC was associated with unknown fractions that could contribute to the observed POM ratios. Thus, the elemental composition of plankton biomass and associated community structure and physiology appear to be the main drivers of particulate organic matter concentrations and ratios in this area, but there are likely periods where other sources of particulate matter are important. *Prochlorococcus* and *Synechococcus* cells have been shown to have elevated elemental ratios (Bertilsson et al. 2003; Martiny et al. 2013a) and likely contribute to the higher ratios observed during the summer and fall. However, the biomass analysis shows that *Prochlorococcus* and *Synechococcus* are a small proportion of the total POC stock. This limited contribution by Cyanobacteria to overall biomass suggests that changes in eukaryotic phytoplankton must contribute to the elevated ratios observed during the summer and fall—perhaps as a result of physiological acclimation to nutrient limitation or higher temperature (Rhee 1978; Toseland et al. 2013).

There is increasing evidence that elemental ratios of marine communities are not static but vary regionally depending on the environmental conditions and associated changes in cellular physiologies and community composition. Our study adds to this emerging view and suggests that the elemental composition of marine communities can also

alter rapidly in response to temporal environmental changes. This variable stoichiometry of environments influences a range of marine biogeochemical functions (Deutsch and Weber 2012) and should be an integral component of our understanding of the links between physical, chemical, and biological components of ocean ecosystems.

## References

- Allison, S. D., Y. Chao, J. D. Farrara, S. Hatosy, and A. C. Martiny. 2012. Fine-scale temporal variation in marine extracellular enzymes of coastal southern California. *Front. Microbiol.* **3**. doi:10.3389/fmicb.2012.00301
- Arrigo, K. R., R. B. Dunbar, M. P. Lizotte, and D. H. Robinson. 2002. Taxon-specific differences in C/P and N/P drawdown for phytoplankton in the Ross Sea, Antarctica. *Geophys. Res. Lett.* **29**. doi:10.1029/2002GL015277
- Bertilsson, S., O. Berglund, D. M. Karl, and S. W. Chisholm. 2003. Elemental composition of marine *Prochlorococcus* and *Synechococcus*: Implications for the ecological stoichiometry of the sea. *Limnol. Oceanogr.* **48**: 1721–1731. doi:10.4319/lo.2003.48.5.1721
- Biondi, F., A. Gershunov, and D. R. Cayan. 2001. North Pacific decadal climate variability since 1661. *J. Clim.* **14**: 5–10. doi:10.1175/1520-0442(2001)014<0005:NPDCVS>2.0.CO;2
- Brzezinski, M. A. 1985. The Si-C-N ratio of marine diatoms—interspecific variability and the effect of some environmental variables. *J. Phycol.* **21**: 347–357.
- Casey, J. R., J. P. Aucan, S. R. Goldberg, and M. W. Lomas. 2013. Changes in partitioning of carbon amongst photosynthetic pico- and nano-plankton groups in the Sargasso Sea in response to changes in the North Atlantic Oscillation. *Deep-Sea Res. Part II Top. Stud. Oceanogr.* **93**: 58–70. doi:10.1016/j.dsr2.2013.02.002
- Chatfield, C. 2013. *The analysis of time series: An introduction*. CRC press.
- Church, M. J., M. W. Lomas, and F. Muller-Karger. 2013. Sea change: Charting the course for biogeochemical ocean time-series research in a new millennium. *Deep-Sea Res. Part II Top. Stud. Oceanogr.* **93**: 2–15. doi:10.1016/j.dsr2.2013.01.035
- Deutsch, C., and T. Weber. 2012. Nutrient ratios as a tracer and driver of ocean biogeochemistry. *Ann. Rev. Mar. Sci.* **4**: 113–141. doi:10.1146/annurev-marine-120709-142821
- Goldman, J. C., J. J. Mccarthy, and D. G. Peavey. 1979. Growth-rate influence on the chemical composition of phytoplankton in oceanic waters. *Nature* **279**: 210–215. doi:10.1038/279210a0
- Goldman, J. C., and M. R. Dennett. 2000. Growth of marine bacteria in batch and continuous culture under carbon and nitrogen limitation. *Limnol. Oceanogr.* **45**: 789–800. doi:10.4319/lo.2000.45.4.0789
- Hagan, M. T., H. B. Demuth, and M. H. Beale. 1996. *Neural network design*. Boston: Pws Pub., 1996.

- Hatosy, S. M., J. B. H. Martiny, R. Sachdeva, J. Steele, J. A. Fuhrman, and A. C. Martiny. 2013. Beta diversity of marine bacteria depends on temporal scale. *Ecology* **94**: 1898–1904. doi:[10.1890/12-2125.1](https://doi.org/10.1890/12-2125.1)
- Hulburt, E. M., J. H. Ryther, and R. R. L. Guillard. 1960. The phytoplankton of the Sargasso Sea off Bermuda. *J. du Cons.* **25**: 115–128. doi:[10.1093/icesjms/25.2.115](https://doi.org/10.1093/icesjms/25.2.115)
- King, A. L., and K. A. Barbeau. 2011. Dissolved iron and macronutrient distributions in the southern California Current System. *J. Geophys. Res. Ocean.* **116**. doi:[10.1029/2010JC006324](https://doi.org/10.1029/2010JC006324)
- Kudela, R. M., W. P. Cochlan, T. D. Peterson, and C. G. Trick. 2006. Impacts on phytoplankton biomass and productivity in the Pacific Northwest during the warm ocean conditions of 2005. *Geophys. Res. Lett.* **33**. doi:[10.1029/2006GL026772](https://doi.org/10.1029/2006GL026772)
- Legaard, K. R., and A. C. Thomas. 2006. Spatial patterns in seasonal and interannual variability of chlorophyll and sea surface temperature in the California Current. *J. Geophys. Res.* **111**. doi:[10.1029/2005JC003282](https://doi.org/10.1029/2005JC003282)
- Legaard, K. R., and A. C. Thomas. 2007. Spatial patterns of intraseasonal variability of chlorophyll and sea surface temperature in the California Current. *J. Geophys. Res.* **112**. doi:[10.1029/2007JC004097](https://doi.org/10.1029/2007JC004097)
- Leonardos, N., and R. J. Geider. 2004. Effects of nitrate: phosphate supply ratio and irradiance on the C : N : P stoichiometry of *Chaetoceros muelleri*. *Eur. J. Phycol.* **39**: 173–180. doi:[10.1080/0967026042000201867](https://doi.org/10.1080/0967026042000201867)
- Lomas, M. W., A. L. Burke, D. A. Lomas, D. W. Bell, C. Shen, S. T. Dyhrman, and J. W. Ammerman. 2010. Sargasso Sea phosphorus biogeochemistry: An important role for dissolved organic phosphorus (DOP). *Biogeosciences* **7**: 695–710. doi:[10.5194/bg-7-695-2010](https://doi.org/10.5194/bg-7-695-2010)
- Mantua, N. J., and S. R. Hare. 2002. The Pacific decadal oscillation. *J. Oceanogr.* **58**: 35–44. doi:[10.1023/A:1015820616384](https://doi.org/10.1023/A:1015820616384)
- Martiny, A. C., C. T. A. Pham, F. W. Primeau, J. A. Vrugt, J. K. Moore, S. A. Levin, and M. W. Lomas. 2013a. Strong latitudinal patterns in the elemental ratios of marine plankton and organic matter. *Nat. Geosci.* **6**: 279–283. doi:[10.1038/ngeo1757](https://doi.org/10.1038/ngeo1757)
- Martiny, A. C., J. A. Vrugt, F. W. Primeau, and M. W. Lomas. 2013b. Regional variation in the particulate organic carbon to nitrogen ratio in the surface ocean. *Global Biogeochem. Cycles* **27**: 723–731. doi:[10.1002/gbc.20061](https://doi.org/10.1002/gbc.20061)
- Martz, T., U. Send, M. D. Ohman, Y. Takeshita, P. Bresnahan, H. J. Kim, and S. Nam. 2014. Dynamic variability of biogeochemical ratios in the Southern California Current System. *Geophys. Res. Lett.* **41**: 2496–2501. doi:[10.1002/2014GL059332](https://doi.org/10.1002/2014GL059332)
- Menden-Deuer, S., and E. J. Lessard. 2000. Carbon to volume relationships for dinoflagellates, diatoms, and other protist plankton. *Limnol. Oceanogr.* **45**: 569–579. doi:[10.4319/lo.2000.45.3.0569](https://doi.org/10.4319/lo.2000.45.3.0569)
- Menzel, D. W., and J. H. Ryther. 1960. The annual cycle of primary production in the Sargasso Sea off Bermuda. *Deep-Sea Res.* **6**: 351–367. doi:[10.1016/0146-6313\(59\)90095-4](https://doi.org/10.1016/0146-6313(59)90095-4)
- Mouginot, C., A. E. Zimmerman, J. A. Bonachela, H. Fredricks, S. D. Allison, B. A. S. Van Mooy, and A. C. Martiny. 2015. Resource allocation by the marine cyanobacterium *Synechococcus* WH8102 in response to different nutrient supply ratios. *Limnol. Oceanogr.* **60**: 1634–1641. doi:[10.1002/lno.10123](https://doi.org/10.1002/lno.10123)
- Quigg, A., and others. 2003. The evolutionary inheritance of elemental stoichiometry in marine phytoplankton. *Nature* **425**: 291–294. doi:[10.1038/nature01953](https://doi.org/10.1038/nature01953)
- Rebstock, G. A. 2003. Long-term change and stability in the California Current System: Lessons from CalCOFI and other long-term data sets. *Deep-Sea Res. Part II Top. Stud. Oceanogr.* **50**: 2583–2594. doi:[10.1016/S0967-0645\(03\)00124-3](https://doi.org/10.1016/S0967-0645(03)00124-3)
- Rhee, G. Y. 1978. Effects of N-P atomic ratios and nitrate limitation on algal growth, cell composition, and nitrate uptake. *Limnol. Oceanogr.* **23**: 10–25. doi:[10.4319/lo.1978.23.1.0010](https://doi.org/10.4319/lo.1978.23.1.0010)
- Rykaczewski, R. R., and D. M. Checkley. 2008. Influence of ocean winds on the pelagic ecosystem in upwelling regions. *Proc. Natl. Acad. Sci. USA* **105**: 1965–1970. doi:[10.1073/pnas.0711777105](https://doi.org/10.1073/pnas.0711777105)
- Scargle, J. D. 1982. Studies in astronomical time-series analysis .2. Statistical aspects of spectral-analysis of unevenly spaced data. *Astrophys. J.* **263**: 835–853. doi:[10.1086/160554](https://doi.org/10.1086/160554)
- Schnetzer, A., and others. 2013. Coastal upwelling linked to toxic *Pseudo-nitzschia australis* blooms in Los Angeles coastal waters, 2005–2007. *J. Plankton Res.* **35**: 1080–1092. doi:[10.1093/plankt/fbt051](https://doi.org/10.1093/plankt/fbt051)
- Seubert, E. L., and others. 2013. Seasonal and annual dynamics of harmful algae and algal toxins revealed through weekly monitoring at two coastal ocean sites off southern California, USA. *Environ. Sci. Pollut. Res.* **20**: 6878–6895. doi:[10.1007/s11356-012-1420-0](https://doi.org/10.1007/s11356-012-1420-0)
- Sharp, J. H. 1974. Improved analysis for “particulate” organic carbon and nitrogen from seawater. *Limnol. Oceanogr.* **19**: 984–989. doi:[10.4319/lo.1974.19.6.0984](https://doi.org/10.4319/lo.1974.19.6.0984)
- Teng, Y.-C., F. W. Primeau, J. K. Moore, M. W. Lomas, and A. C. Martiny. 2014. Global-scale variations of the ratios of carbon to phosphorus in exported marine organic matter. *Nat. Geosci.* **7**: 895–898. doi:[10.1038/ngeo2303](https://doi.org/10.1038/ngeo2303)
- Toseland, A., and others. 2013. The impact of temperature on marine phytoplankton resource allocation and metabolism. *Nat. Clim. Chang.* **3**: 979–984. doi:[10.1038/nclimate1989](https://doi.org/10.1038/nclimate1989)
- Venrick, E. L. 2012. Phytoplankton in the California Current system off southern California: Changes in a changing environment. *Prog. Oceanogr.* **104**: 46–58. doi:[10.1016/j.pocean.2012.05.005](https://doi.org/10.1016/j.pocean.2012.05.005)

- Weber, T. S., and C. Deutsch. 2010. Ocean nutrient ratios governed by plankton biogeography. *Nature* **467**: 550–554. doi:[10.1038/nature09403](https://doi.org/10.1038/nature09403)
- Zimmerman, A. E., S. D. Allison, and A. C. Martiny. 2014a. Phylogenetic constraints on elemental stoichiometry and resource allocation in heterotrophic marine bacteria. *Environ. Microbiol.* **16**: 1398–1410. doi:[10.1111/1462-2920.12329](https://doi.org/10.1111/1462-2920.12329)
- Zimmerman, A. E., A. C. Martiny, M. W. Lomas, and S. D. Allison. 2014b. Phosphate supply explains variation in nucleic acid allocation but not C : P stoichiometry in the western North Atlantic. *Biogeosciences* **11**: 1599–1611. doi:[10.5194/bg-11-1599-2014](https://doi.org/10.5194/bg-11-1599-2014)

### Acknowledgments

We thank Steven Allison, Stephen Hatossy, Michael Louie, Erik Lee, Matthew Hernandez III, and Michael Lomas for help with the sampling and analysis. Financial support for this work was provided by the National Science Foundation Dimensions of Biodiversity (OCE-1046297) and Major Research Instrumentation programs (OCE-1126749) (to ACM), NSF Dimensions of Biodiversity (OCE-1136818) and National Oceanic and Atmospheric Administration subaward NA08OAR4320894 (to DAC), and the Undergraduate Research Opportunities Program at UCI (to JL and JH).

*Submitted 2 June 2015*

*Revised 8 September 2015*

*Accepted 29 October 2015*

*Associate editor: Anya Waite*